

## Electronic Supplementary Information

**Constructing a magnetic ionic covalent organic polymer through post-synthesis  
functionalization approach for efficient iodine/iodide adsorption**

Yang Shen, Jingbo Zhang, Yue Wang, Xuemei Li\*

*School of Chemical and Pharmaceutical Engineering, Jilin Institute of Chemical  
Technology 132022, China*

\*Corresponding author: E-mail: lixuemei@jlict.edu.cn.

## 1. Characterization

Fourier Transform Infrared Spectroscopy (FT-IR) was used to determine the structure and surface functional groups (model: PE Frontier NIR, America). The images from the scanning electron microscope (SEM) were captured using a Thermo Scientific microscope (model: Apreo 2, America). The images transmission electron microscopy (TEM) were captured using a Thermo Scientific microscope (model: JEM-2100F, Jeol Ltd., Japan) after the specimens were dispersed in ethanol and placed on holey copper grids. The thermal stability of the samples was measured using a thermogravimetric (TGA) analyzer (model: Discovery SDT650, America) by scanning from ambient temperature to 800°C at a heating rate of 10°C min<sup>-1</sup> under nitrogen atmosphere. The X-ray photoelectron spectroscopy (XPS) was recorded using a Thermo Fisher Scientific (model: Shimadzu/Krayos AXIS Ultra DLD, Japan) to study the form of adsorbed molecule iodine. Ultraviolet-visible (UV-Vis) spectroscopic analyses were performed on a Persee UV-Vis spectrophotometer (model: T-9, Beijing). Raman spectra were acquired using a HORIBA JobinYvon Aramis equipped with a 532 nm diode laser (model: Lab RAM HR Evolution, France). The magnetic properties of the sample were tested at ambient temperature using a vibrating sample magnetometer (VSM) (model: LakeShore7404, America). The specific surface areas were evaluated by Micromeritics instrument (model: ASAP 2020, America). The CPMAS <sup>1</sup>H and <sup>13</sup>C NMR measurements were carried out with spectrometer operating at 400 and 101 MHz, respectively (model: Bruker AVANCE NEO500M, Germany).

## 2. Uptake of iodine

### 2.1. Iodine vapor adsorption capacity

$$Q_t = \frac{(m_t - m_1) - (m_{r,t} - m_{r,0})}{m_1 - m_0} \quad (\text{S1})$$

Where  $Q_t$  ( $\text{g g}^{-1}$ ) is the static  $I_2$  uptake capacity at time  $t$ ,  $m_t$  (g) is the weight of the third vial at time  $t$ ,  $m_1$  is the weight of the third vial before the adsorption experiment,  $m_0$  is the weight of first vial without IMF-COP-Fe,  $m_{r,t}$  is the weight of the second vial at time  $t$ ,  $m_{r,0}$  is the weight of second vial before the adsorption experiment.

### 2.2. Equations of adsorption capacity

$$Q_t = \frac{(C_0 - C_t)V}{m} \quad (\text{S2})$$

Where  $Q_t$  ( $\text{mg g}^{-1}$ ) is the equilibrium capacity of IMF-COP-Fe for iodine/iodide;  $C_0$  ( $\text{mg L}^{-1}$ ) is the initial concentration of the iodine-cyclohexane solution (iodide solution);  $C_t$  ( $\text{mg L}^{-1}$ ) is the concentration of iodine-cyclohexane solution (iodide solution) when the adsorption time is  $t$ ;  $m$  (g) is the mass of IMF-COP-Fe;  $V$  (L) indicates the iodine-cyclohexane solution (iodide solution) volume.

### 2.3. Adsorption kinetics and the internal diffusion models

$$\ln(Q_e - Q_t) = \ln Q_e - k_1 t \quad (\text{S3})$$

$$\frac{t}{Q_t} = \frac{1}{k_2 Q_e^2} + \frac{t}{Q_e} \quad (\text{S4})$$

$$Q_t = K_p t^{0.5} + C \quad (\text{S5})$$

Where  $k_1$  ( $\text{min}^{-1}$ ) and  $k_2$  ( $\text{g mg}^{-1} \text{ min}^{-1}$ ) are the kinetic constants of the pseudo-first-order and pseudo-second-order kinetic model, the adsorbed amount of iodine is  $Q_e$  ( $\text{mg g}^{-1}$ ) at equilibrium and  $Q_t$  ( $\text{mg g}^{-1}$ ) at  $t$  (min).

## 2.4. Langmuir and Freundlich models

$$\frac{C_e}{Q_e} = \frac{C_e}{Q_0} + \frac{1}{Q_0 K_c} \quad (S6)$$

$$\ln Q_e = \ln K_F + \frac{1}{n} \ln C_e \quad (S7)$$

The equilibrium adsorption capacity of IMF-COP-Fe is denoted by  $Q_e$  ( $\text{mg g}^{-1}$ ).

$C_e$  ( $\text{mg L}^{-1}$ ) is the concentration of iodide in the solution at equilibrium for IMF-COP-Fe.  $Q_0$  ( $\text{mg g}^{-1}$ ) is the theoretical maximum adsorption capacity based on the Langmuir model. The adsorption intensity coefficient is denoted by  $n$ , while  $K_c$  and  $K_F$  represent the adsorption equilibrium coefficients for the Langmuir and Freundlich models, respectively.

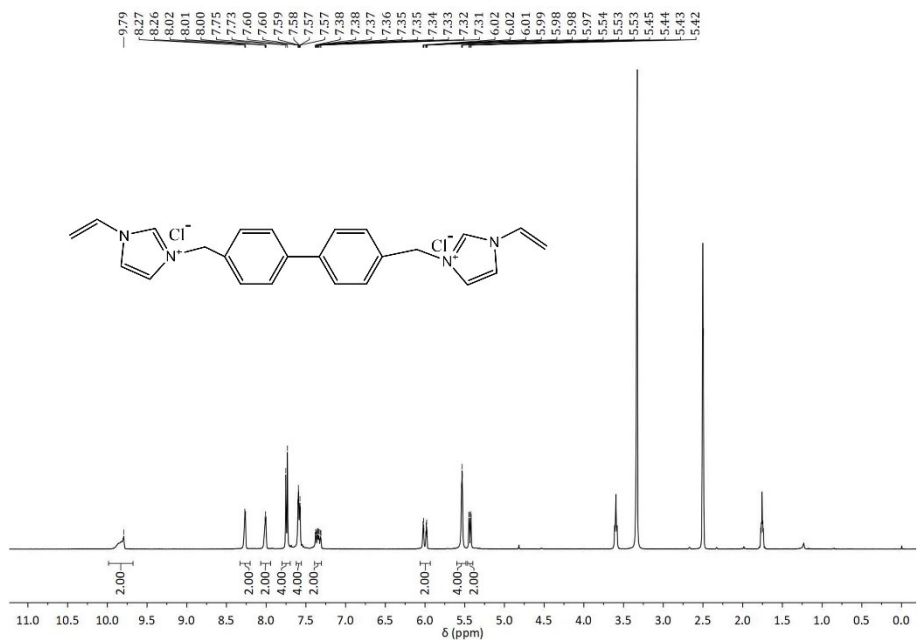


**Fig. S1**  $^1\text{H}$  NMR (400 MHz, DMSO-d6)  $\delta$  9.79 (s, 2H), 8.26 (d,  $J$  = 3.1 Hz, 2H), 8.07 – 7.94 (m, 2H), 7.74 (d,  $J$  = 8.1 Hz, 4H), 7.62 – 7.56 (m, 4H), 7.39 – 7.30 (m, 2H), 6.06 – 5.93 (m, 2H), 5.60 – 5.48 (m, 4H), 5.43 (dd,  $J$  = 8.8, 2.4 Hz, 2H).

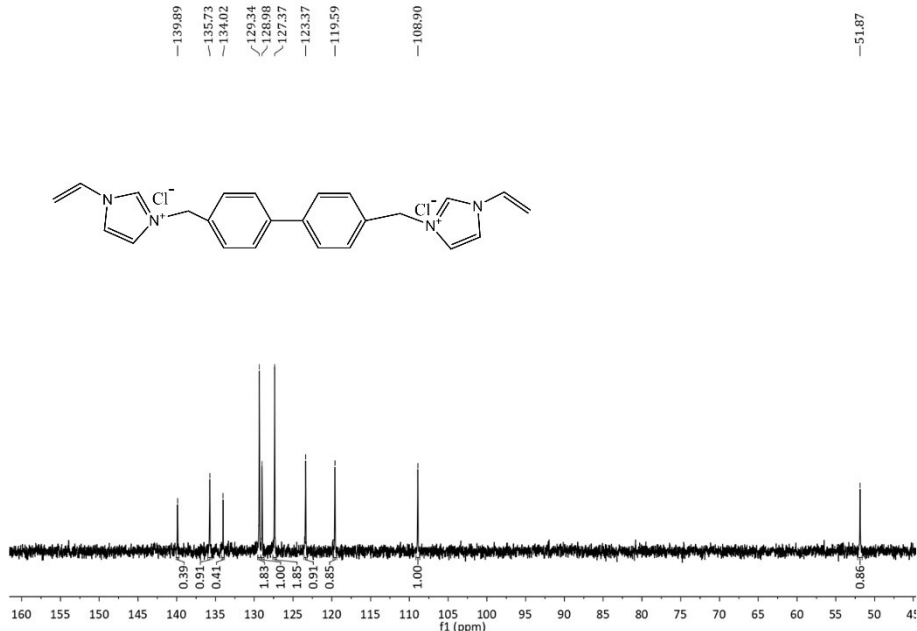


**Fig. S2**  $^{13}\text{C}$  NMR (101 MHz, DMSO-d6)  $\delta$  139.89, 135.73, 134.02, 129.34, 128.98, 127.37, 123.37, 119.59, 108.90, 51.87.

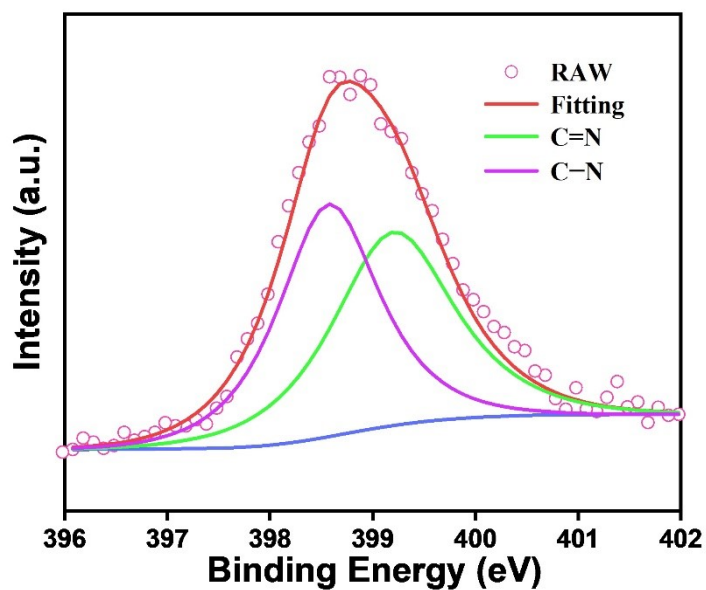


**Fig. S3** N 1s XPS spectra of COP.

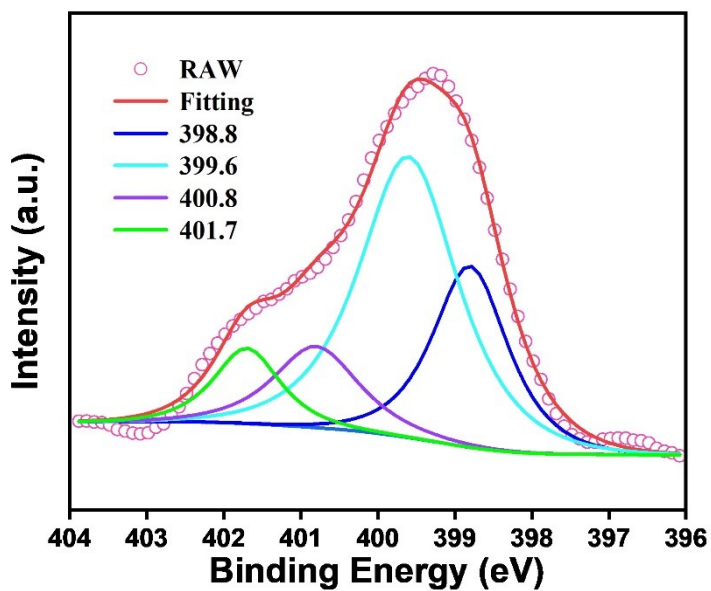


**Fig. S4** N 1s XPS spectra of IMF-COP-Fe.

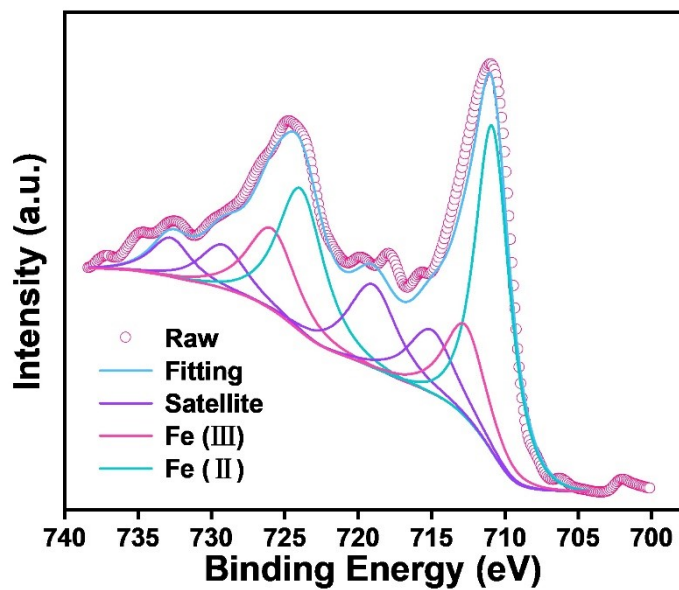


**Fig.S5** Fe 2p XPS spectra of IMF-COP-Fe.

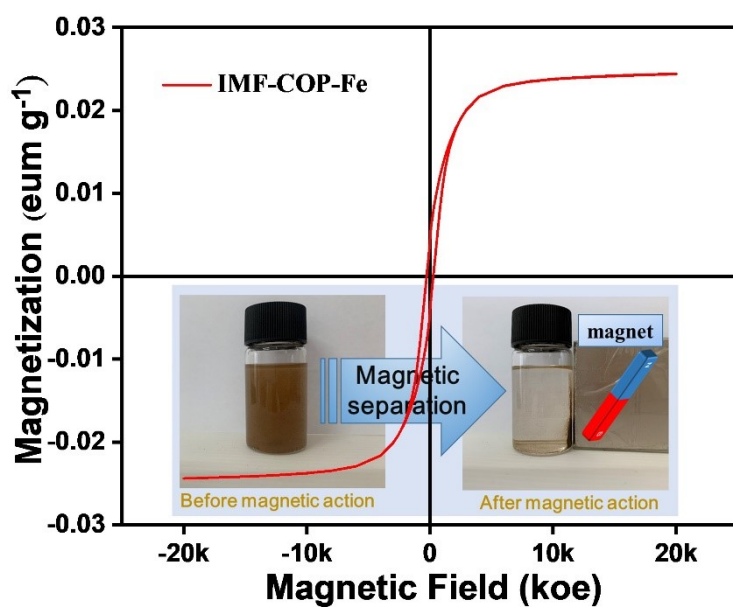


**Fig. S6** VSM from the IMF-COP-Fe (inset: magnetic separation of IMF-COP-Fe from cyclohexane solution under an external magnet).

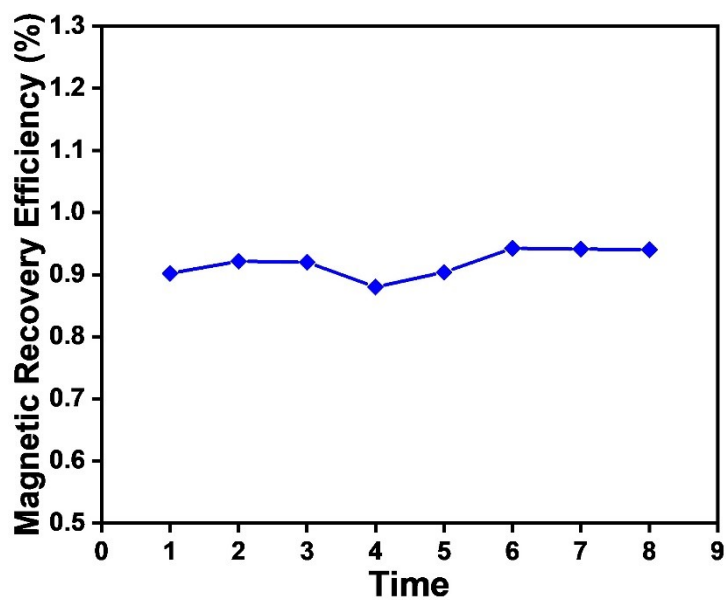


**Fig. S7** The magnetic recovery efficiency of IMF-COP-Fe.

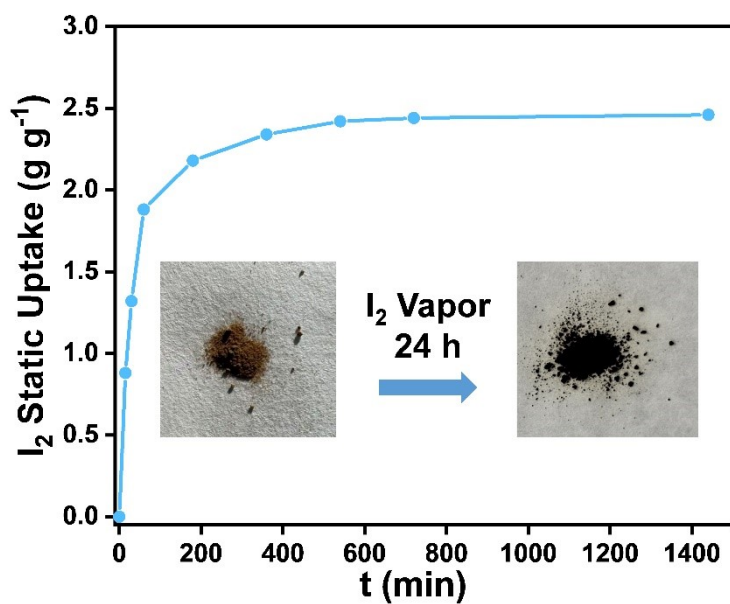


**Fig. S8** Static I<sub>2</sub> vapor adsorption kinetics on IMF-COP-Fe upon exposure to I<sub>2</sub> vapor at 75°C.

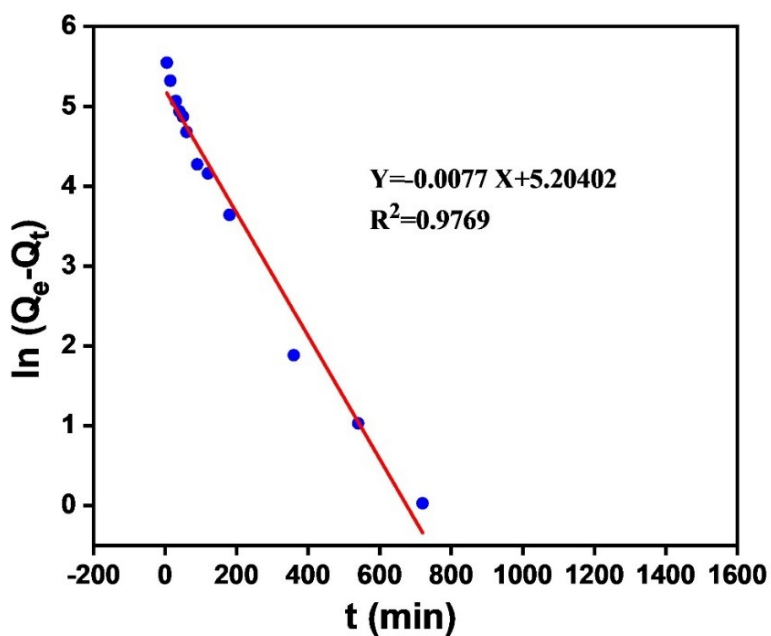


**Fig. S9** Pseudo-first-order kinetic model of iodine uptake on IMF-COP-Fe.

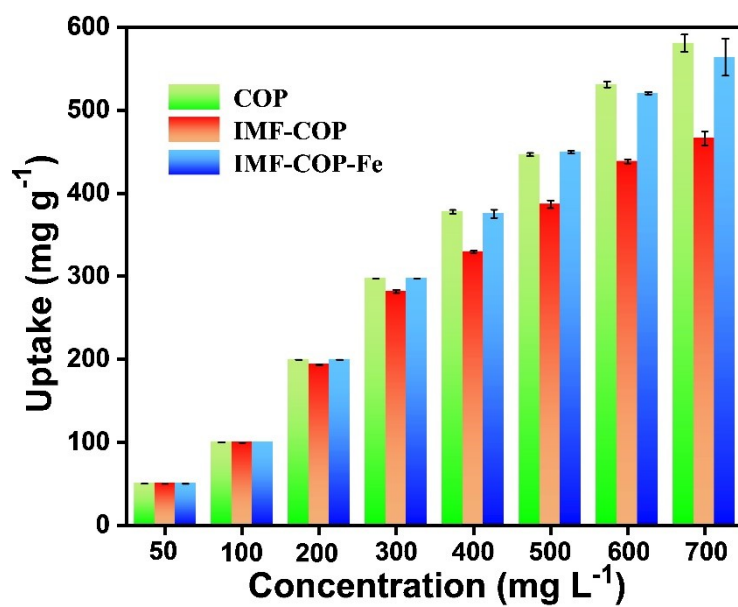


**Fig. S10** The maximum adsorption capacity of COP, IMF-COP and IMF-COP-Fe at different concentrations of iodine-cyclohexane solution.

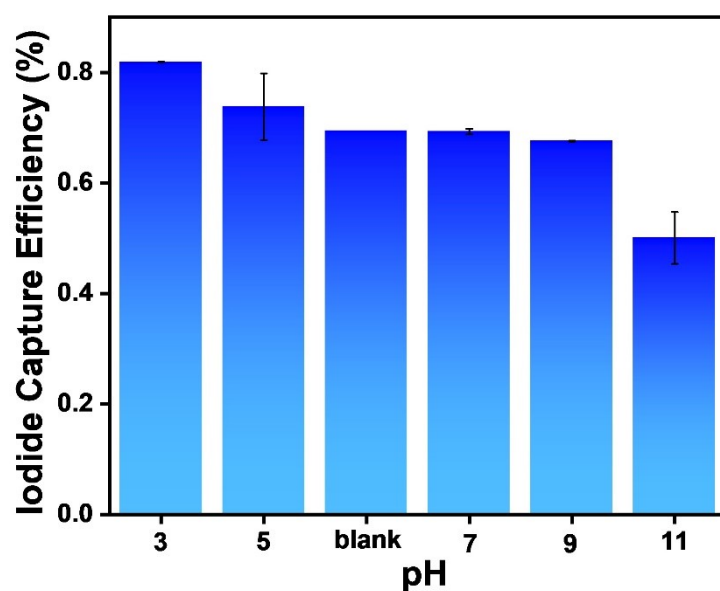


**Fig. S11** Effect of pH on iodide removal efficiency of IMF-COP-Fe.

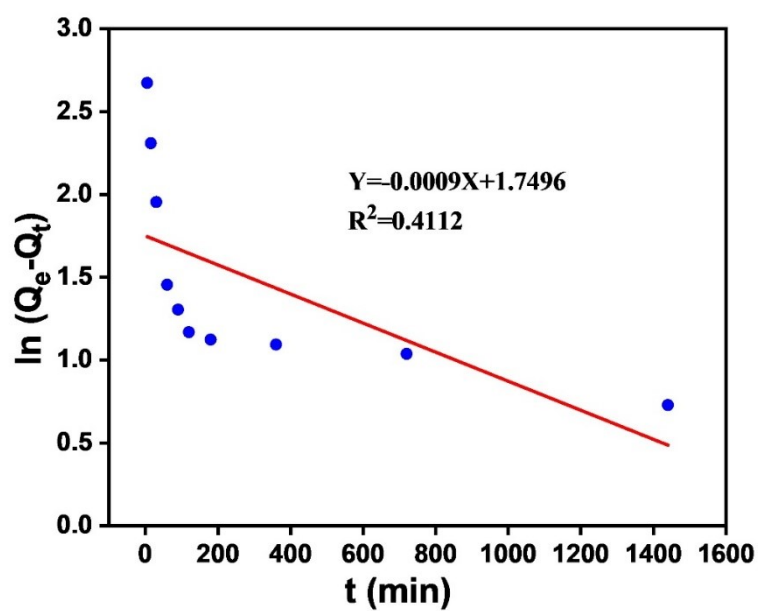


**Fig. S12** Pseudo-first-order kinetic model of iodide uptake on IMF-COP-Fe.

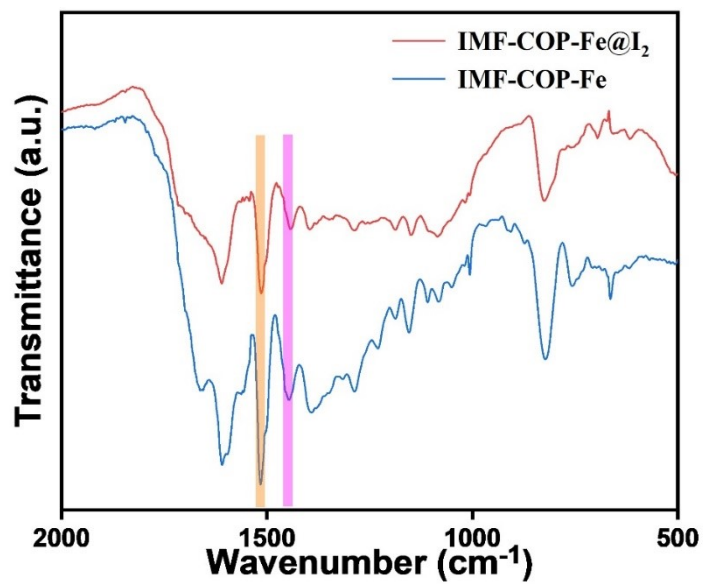


**Fig. S13** The FT-IR analysis of IMF-COP-Fe and IMF-COP-Fe@I<sub>2</sub>.

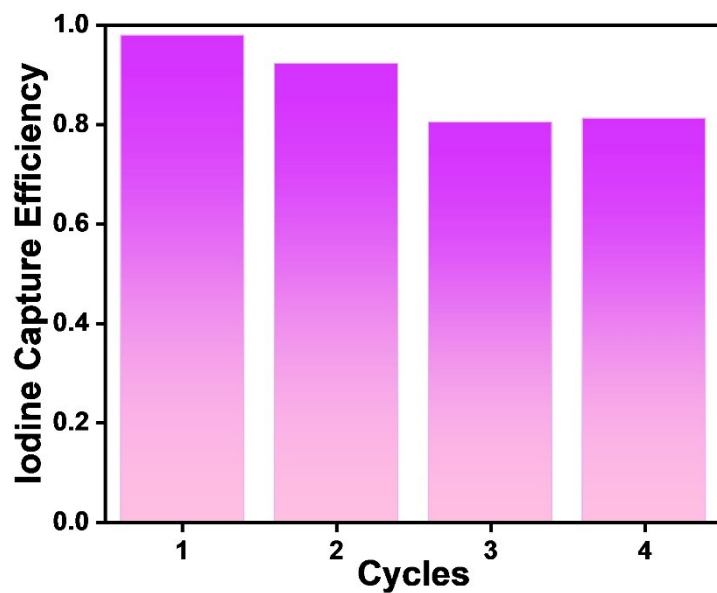


**Fig. S14** Recycling test for IMF-COP-Fe adsorption on iodine.

**Table S1** Pseudo-first-order and pseudo-second-order model parameters of adsorption iodine for IMF-COP-Fe.

Adsorbent	Pseudo-first-order model			Pseudo-second-order model		
	Q <sub>e</sub>	k <sub>1</sub>	R <sup>2</sup>	Q <sub>e</sub>	k <sub>2</sub>	R <sup>2</sup>
	(mg g <sup>-1</sup> )	(min <sup>-1</sup> )		(mg g <sup>-1</sup> )	(g mg <sup>-1</sup> min <sup>-1</sup> )	
IMF-COP-Fe	182.00	0.0077	0.9769	414.94	0.0001167	0.9999

**Table S2** Pseudo-first-order and pseudo-second-order model parameters of adsorption iodide for IMF-COP-Fe.

Adsorbent	Pseudo-first-order model			Pseudo-second-order model		
	Q <sub>e</sub>	k <sub>1</sub>	R <sup>2</sup>	Q <sub>e</sub>	k <sub>2</sub>	R <sup>2</sup>
	(mg g <sup>-1</sup> )	(min <sup>-1</sup> )		(mg g <sup>-1</sup> )	(g mg <sup>-1</sup> min <sup>-1</sup> )	
IMF-COP-Fe	5.75	0.0009	0.4112	77.58	0.02163	0.9999

**Table S3** Textural properties of different samples.

sample	S <sub>BET</sub> <sup>a</sup> (m <sup>2</sup> ·g <sup>-1</sup> )	V <sub>p</sub> <sup>b</sup> (cm <sup>3</sup> ·g <sup>-1</sup> )	D <sub>av</sub> <sup>c</sup> (nm)
COP	37.10	0.074	7.97
IMF-COP	18.86	0.042	8.99
IMF-COP-Fe	22.10	0.059	10.76

<sup>a</sup> Surface area calculated from N<sub>2</sub> adsorption isotherms using the BET equation.

<sup>b</sup> Pore volume calculated from nitrogen uptake at p/p<sub>0</sub> = 0.99.

<sup>c</sup> Average pore size.

**Table S4** The comparison of iodine uptake capacities with other reported adsorbent materials.

Adsorbent	Category	Guest molecules	Adsorption capacity(mg g <sup>-1</sup> )	Ref.
T_COP-1	COPs	I <sub>2</sub>	1045	1
T_COP-2	COPs	I <sub>2</sub>	970	1
T_COP-3	COPs	I <sub>2</sub>	950	1
SIOC-COF-7	COFs	I <sub>2</sub>	1270	2
mICOP-1@agar	COPs	I <sub>2</sub>	1152.5	3
ICOP-1	COPs	I <sub>2</sub>	695.5	3
P-COFs	COFs	I <sub>2</sub>	1300	4
PIPCOP	COPs	I <sub>2</sub>	1950	5
PT-POP	POPs	I <sub>2</sub>	340	6
DaTd-COF	COFs	I <sub>2</sub>	666.79	7
P-TzTz	POPs	I <sub>2</sub>	494.09	8
SCNU-Z4	MOFs	I <sub>2</sub>	332	9
Mxene-PILs	Composites (PILs)	I <sub>2</sub>	170	10
Th-MOF	MOFs	I <sub>2</sub>	1046	11
PHCPs	HCPs	I <sub>2</sub>	469	12
AZO-TPA	Composites	I <sub>2</sub>	661.79	13
AZO-TPA-600	Composites	I <sub>2</sub>	775.36	13
UA-DT	Composites	I <sub>2</sub>	334.5	14
Complexes 1	Composites	I <sub>2</sub>	638.5	15
nano Cu <sub>2</sub> O/Cu-C	Composites	I <sup>-</sup>	41.2	16

$\text{Cu}_{0.1}\text{Zn}_{0.9}@\text{NC}$	Composites	$\text{I}^-$	(pH=3) 235.5	17
$\text{Ag}^0\text{-UiO-66-(OH)}_2$	Composites	$\text{I}^-$	531.98	18
$\text{Ag}^+@\text{UiO-66-(COOH)}_2$	MOFs	$\text{I}^-$	235.5	19
MXene-PDA- $\text{Bi}_6\text{O}_7$	Composites	$\text{I}^-$	64.65	20
$\beta\text{-Bi}_2\text{O}_3$	Metal oxides	$\text{I}^-$	239.5	21
$\sigma\text{-Bi}_2\text{O}_4@\text{PES}$	Composites	$\text{I}^-$	95.4	22
Purolite A530E	Resins	$\text{I}^-$	275.16	23
HDPy-bent	Composites	$\text{I}^-$	80	24
Hal/ $\text{Ag}_2\text{O}$ -2	Composites	$\text{I}^-$	57.5	25
Cu/ $\text{Al}_2\text{O}_3$ aerogels	Aerogels	$\text{I}^-$	407.6	26
Alg-BO	Composites	$\text{I}^-$	111.8	27
SiPyR-N4	Resins	$\text{I}^-$	124	28
CMPs-1	CMPs	$\text{I}^-$	(t=10°C) 16.93	29
CAU-17	Composites	$\text{I}^-$	268.9	30
PGM220%- $\text{Ag}^+$	Composites	$\text{I}^-$	100.82	31
IMF-COP-Fe	Composites (ILs)	$\text{I}_2/\text{I}^-$	563.92(700 mg L <sup>-1</sup> )/109.90	This work

## References

- 1 A. Hassan, A. Alam, M. Ansari and N. Das, *Chem. Eng. J.*, 2022, **427**, 130950.
- 2 Z. J. Yin, S. Q. Xu, T. G. Zhan, Q. Y. Qi, Z. Q. Wu and X. Zhao, *Chem. Commun.*, 2017, **53**, 7266-7269.
- 3 Q. Tao, L. Sun and L. Jing, *Sep. Purif. Technol.*, 2025, **353**, 128608.
- 4 Y. Li, X. Li, J. Li, W. Liu, G. Cheng and H. Ke, *Microporous Mesoporous Mater.*, 2021, **325**, 111351.
- 5 W. Lu, Y. Zhao and B.-W. Sun, *J. Solid State Chem.*, 2024, **336**, 124724.
- 6 F. Khosravi Esmaeiltarkhani, M. Dinari and N. Mokhtari, *New J. Chem.*, 2024, **48**, 1943-1951.
- 7 Z. Wu, W. Wei, J. Ma, J. Luo, Y. Zhou, Z. Zhou and S. Liu, *ChemistrySelect*, 2021, **6**, 10141-10148.
- 8 X. Pan, C. Ding, Z. Zhang, H. Ke and G. Cheng, *Microporous Mesoporous Mater.*, 2020, **300**, 110161.
- 9 G. Wang, J. Huang, X. Huang, S. Deng, S. Zheng, S. Cai, J. Fan and W. Zhang, *Inorg. Chem. Front.*, 2021, **8**, 1083-1092.
- 10 S. Sun, X. Sha, J. Liang, G. Yang, X. Hu, Z. He, M. Liu, N. Zhou, X. Zhang and Y. Wei, *J. Hazard. Mater.*, 2021, **420**, 126580.
- 11 Y. Ju, Z. J. Li, J. Qiu, X. Li, J. Yang, Z. H. Zhang, M. Y. He, J. Q. Wang and J. Lin, *Inorg. Chem.*, 2023, **62**, 8158-8165.
- 12 J. Ma, Z. Shi, T. Wang, X. Huang, Y. Zhao, J. Wang, J. Li, D. Wang, L. Sun, G. Dong and M. Zhao, *ACS Sustainable Chem. Eng.*, 2024, **12**, 12113-12125.
- 13 X. Zhu, H. Li, Z. Sun, J. Wan, Y. Xin, W. Li, J. Luan and Y. Liu, *Carbon*, 2024, **226**, 119232.
- 14 Z. Shi, X. Huang, Y. Zhao, J. Li, Y. Q. Tian, P. P. Zhang, M. Zhu and M. Zhao, *Environ. Res.*, 2023, **235**, 116617.
- 15 M. Y. Sun, F. Y. Bai, Q. L. Guan, Y. H. Xing and F. Xu, *CrystEngComm*, 2022, **24**, 8309-8320.
- 16 X. Zhang, P. Gu, X. Li and G. Zhang, *Chem. Eng. J.*, 2017, **322**, 129-139.
- 17 J. Chen, P. Wang, C. Gong, Y. Sun, B. Zhu, Y. Yang and F. Liu, *J. Environ. Chem. Eng.*, 2024, **12**, 112235.
- 18 T. Wang, H. Zhao, X. Zhao and D. Liu, *J. Solid State Chem.*, 2022, **305**, 122680.
- 19 J. Zhang, S. Yang, L. Shao, Y. Ren, J. Jiang, H. Wang, H. Tang, H. Deng and T. Xia, *Molecules*, 2022, **27**, 8547.
- 20 X. Sha, H. Huang, S. Sun, H. Huang, Q. Huang, Z. He, M. Liu, N. Zhou, X. Zhang and Y. Wei, *J. Environ. Chem. Eng.*, 2020, **8**, 104261.
- 21 L. Xu, P. Lin, Y. Gao, Y. Qin, Z. Xu and F. Liu, *Sep. Purif. Technol.*, 2022, **292**, 121045.
- 22 Q. Zhao, G. Chen, Z. Wang, M. Jiang, J. Lin, L. Zhang, L. Zhu and T. Duan, *Chem. Eng. J.*, 2021, **426**, 131629.
- 23 Y. Zhao, J. Li, L. Chen, Q. Guo, L. Li, Z. Chai and S. Wang, *J. Radioanal. Nucl. Chem.*, 2023, **332**, 1193-1202.
- 24 J. Yang, W. Tai, F. Wu, K. Shi, T. Jia, Y. Su, T. Liu, P. Mocilac, X. Hou and X. Chen, *Chemosphere*, 2022, **292**, 133401.

- 25 W. Yu, Q. Dong, W. Yu, Z. Qin, X. Nie, Q. Wan and X. Chen, *Minerals*, 2022, **12**, 304.
- 26 X. Zhou, P. Mao, H. Jin, W. Huang, A. Gu, K. Chen, S. Yun, J. Chen and Y. Yang, *J. Hazard. Mater.*, 2023, **443**, 130349.
- 27 T. Kim, C. Seo, J. Seon, A. Battulga and Y. Hwang, *Int. J. Mol. Sci.*, 2022, **23**, 12225.
- 28 Z. Ye, L. Chen, C. Liu, S. Ning, X. Wang and Y. Wei, *React. Funct. Polym.*, 2019, **135**, 52-57.
- 29 R. Jiao, Y. Si, W. Fan, H. Sun, J. Li, Z. Zhu and A. Li, *Sep. Purif. Technol.*, 2025, **353**, 128561.
- 30 Y. Xiong, P. Zhang, W. Ren, S. Li and C. Jin, *J. Environ. Chem. Eng.*, 2024, **12**, 111906.
- 31 X. Pan, M. Jin, J. Zu, G. Han, J. Diao, S. Liu and Q. Tang, *Sep. Purif. Technol.*, 2024, **345**, 127287.